

Time-resolved surface scattering imaging of organic liquids under femtosecond KrF laser pulse excitation

著者	福村 裕史
journal or publication title	Applied Physics Letters
volume	73
number	24
page range	3498-3500
year	1998
URL	http://hdl.handle.net/10097/35100

doi: 10.1063/1.122816

Time-resolved surface scattering imaging of organic liquids under femtosecond KrF laser pulse excitation

Koji Hatanaka

Department of Applied Physics, Osaka University, Suita, Osaka 565-0871, Japan and Advanced Photon Research Center, Kansai Research Establishment, Japan Atomic Energy Research Institute, Neyagawa, Osaka 572-0019, Japan

Tamitake Itoh

Advanced Photon Research Center, Kansai Research Establishment, Japan Atomic Energy Research Institute, Neyagawa, Osaka 572-0019, Japan

Tsuyoshi Asahi

Department of Applied Physics, Osaka University, Suita, Osaka 565-0871, Japan

Nobuyuki Ichinose, Shunichi Kawanishi, and Tsuneo Sasuga

Advanced Photon Research Center, Kansai Research Establishment, Japan Atomic Energy Research Institute, Neyagawa, Osaka 572-0019, Japan

Hiroshi Fukumura^{a)} and Hiroshi Masuhara^{b)}

Department of Applied Physics, Osaka University, Suita, Osaka 565-0871, Japan

(Received 22 July 1998; accepted for publication 9 October 1998)

Time-resolved surface scattering imaging was performed for liquid benzyl chloride and liquid toluene under femtosecond KrF laser ablation conditions. No scattering image was obtained until 1 ns, while scattering started from 2 ns when the laser fluence exceeded 25 mJ/cm², and its intensity increased with the passage of time. The higher the laser fluence was, the steeper the increasing slope was. The scattering is due to surface roughness, which is the initial stage of macroscopic morphological changes. Root-mean-square surface roughness was estimated from the scattering intensity by using frosted fused-silica plates as reference samples. The induced surface roughness increases to a few hundred nm in 10 ns. © 1998 American Institute of Physics.

[S0003-6951(98)02150-0]

Intense laser pulse irradiation onto condensed matters inevitably leads to macroscopic morphological changes such as etching, pit formation, and melting. In order to obtain some clues to clarify their primary processes leading to morphological changes, various kinds of dynamic surface observation methods have been developed and applied so far. Time-resolved measurements *in situ* are indeed indispensable to obtain detailed information on the dynamics of morphological changes and to elucidate their microscopic mechanism, in addition to static observation methods such as scanning electron microscopy, and so on.

Time-resolved shadowgraphy was carried out to observe the phenomena induced above a sample surface such as shockwave expansion and plume ejection, and to determine ablation threshold values, where its spatial and temporal resolutions are, typically, $\sim 10 \mu\text{m}$ and 20 ns, respectively.¹ Time-resolved interferometry was also performed to analyze the whole surface expansion and contraction dynamics of polymer films,² where its spatial and temporal resolutions are $\sim 30 \text{ nm}$ and 8 ns, respectively. Furthermore, in the ps time domain, time-resolved surface reflectance imaging was performed on the surface of Si,³ and so on. This method mainly focuses on the reflectivity change and the attenuation of a

probe light pulse by ejected materials, not on the surface morphology.

Noncontact time-resolved observation methods such as those described above enable us to adopt liquids as an ablation target. Because a liquid surface is too soft for mechanical measurements, their morphological changes are always transient, and their flat surfaces recover quickly. In fact, we have already succeeded in the clarification of morphological change dynamics of liquid benzene derivatives induced by a ns KrF laser pulse irradiation with time-resolved shadowgraphy in the time range from tens of ns to hundreds of μs .⁴ The molecular photochemical mechanism of the liquid ablation was elucidated by comparing the dynamics with transient absorption and emission spectroscopic analyses. To bridge the macroscopic dynamics and microscopic mechanism, surface roughness induced priorly to shockwave generation, plume ejection, surface elevation, and so on, should be made clear.

Based on the background described above, in this letter an ultrafast surface scattering imaging method is developed and applied to clarify the initial stage of morphological changes induced on a liquid surface with higher spatial and temporal resolutions. An experimental setup is shown in Fig. 1. As an excitation light pulse, a fs ultraviolet laser pulse (248 nm, 300 fs) from a high-power fs KrF laser system irradiates a free surface of a sample liquid in a fused-silica container (3 cm diam, 5 mm deep) via a lens ($f=30 \text{ cm}$)

^{a)}Present address: Department of Chemistry, Graduate School of Chemistry,

^{b)}Electronic mail: masuhara@ap.eng.osaka-u.ac.jp

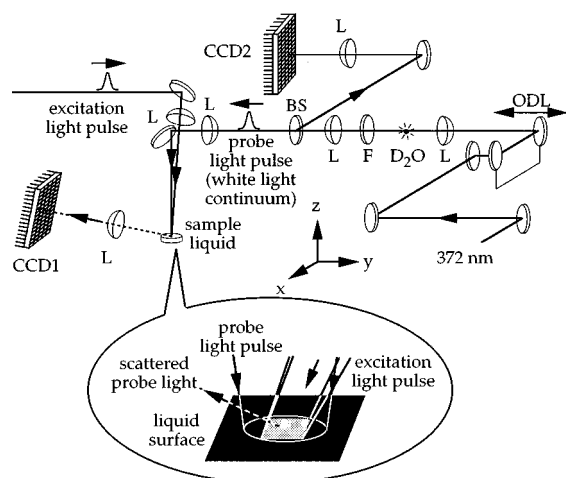


FIG. 1. An experimental setup for time-resolved surface scattering imaging. L; lens, ODL; optical delay line, D₂O; 1 cm path length D₂O cell, F; filter, BS; beam splitter, and CCD1(2); charge-coupled device for measurement (fluctuation monitoring).

with a spot size of $1 \times 1 \text{ mm}^2$. Laser intensity is variable by the use of partially transmitting attenuators and measured by a joule meter (Gentec, ED-500 or Lasertechnik Berlin, PEM100). Laser fluence F is calculated by the equation of $F = \text{laser intensity}/\text{spot size}$. A white light continuum is obtained by focusing a second harmonic (150 fs, 372 nm, 10 Hz) from the laser system into a 1 cm path length D₂O cell after a variable optical delay line (19 ns at the longest) and used as a probe light pulse to take a scattering image on a sample liquid surface by a charge-coupled device (Sony, XC-7500)(CCD1). Here, the D₂O cell is used as a wavelength converter because the CCD does not have a sensitivity at 372 nm. The observation peak wavelength is set to 460 nm considering the sensitivity of CCD1. The probe light pulse is incident on a liquid surface vertically downward. The observing angle is $\sim 60^\circ$ to the liquid normal and its solid angle is $2^2\pi/13^2$ sr. At the same time, another CCD (CCD2) is set to monitor the intensity fluctuation of white light continuum. The time origin is determined by measuring a transient absorption spectrum of liquid benzyl chloride. The effective pulse width is < 6 ps taking optical chirp into consideration. With this method, the time resolution is in the order of ps and the spatial resolution is estimated to be comparable to that of the interferometry (~ 30 nm).² It is important in this experimental system that images can be obtained only when the surface roughness is induced. If no morphological change is induced on the surface, the white light continuum never reaches the CCD. Sample liquids are benzyl chloride (refractive index at 460 nm, $n_{460} = 1.53$, 99%, Nacalai Tesque) and toluene ($n_{460} = 1.49$, 99%, Nacalai Tesque). The samples are used after N₂ bubbling for several minutes. Experiments are performed at 294 K under atmospheric pressure.

A typical example of sequential scattering images is shown in Fig. 2, where the sample liquid is toluene and $F = 90 \text{ mJ/cm}^2$. No scattering images are obtained until 1 ns. At ~ 2 ns the scattering from the irradiated area is obtained and its intensity increases with the passage of time. The light and shade in the irradiated spot are due to the spatial intensity irregularity of an excitation light pulse. This transient behavior indicates that the surface scattering is induced by

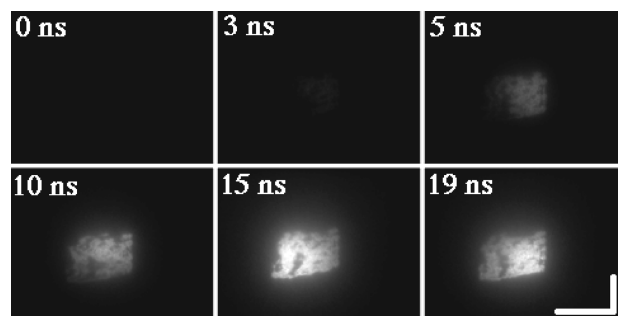


FIG. 2. Scattering images obtained by CCD1 in Fig. 1 when the sample liquid is toluene and $F = 90 \text{ mJ/cm}^2$. The time in each frame represents a delay time. The vertical and horizontal white bars in the last frame represent 1 mm.

surface morphological changes, not by a transient refractive index change. This is confirmed by fs absorption spectroscopy under the same condition which is conducted separately in our laboratory.⁵ Transient absorption of molecular excited states (monomer and excimer absorption bands, and so on), which may lead to the refractive index change, was observed already at 0 ns. Furthermore, a broadband whose absorbance intensity decreases in the longer wavelength of 300–500 nm was observed in the same ns time domain, and its absorbance intensity increased with the same passage of time. This tailing component is usually ascribed to the scattering of a probe light pulse. The surface morphological change is considered to be laser-induced surface roughness, while a flat surface displacement due to the expansion/contraction of liquids does not induce such scattering.

Here, the scattering intensity (CCD1) is corrected to the reference intensity (CCD2) because the intensity of a probe light pulse fluctuates shot by shot, and the corrected scattering intensity I_{scat} is plotted against the delay time. The results are summarized as a function of fluence in Fig. 3. When the laser fluence is relatively low ($F = 10 \text{ mJ/cm}^2$), there is no scattering obtained until 19 ns. As the laser fluence increases higher than 25 mJ/cm^2 , however, the scattering intensity is counted remarkably. When the scattering starts are dependent on F , the higher the fluence is, the earlier the starting time is. This tendency reminds us of a similar correlation in the conventional shadowgraphy of the same liquids⁶ where the spatial resolution is $\sim 10 \mu\text{m}$. Furthermore, the intensity increasing slope is also dependent on F ; the higher the laser fluence is, the acceleratively steeper the increasing slope is. This may be due to the difference of the initial amount of transient species such as benzyl radicals⁷ leading to the surface roughness. In the case of higher F , saturation and fluctuation of scattering intensity are observed at the late stage, which may be due to the fact that ejected plumes detached from a liquid surface shut out the incident probe light pulse, and its intensity reaching a liquid surface is decreased as a result. This attenuation effect was also presented in a ps reflectance imaging of Si.³ The scattering intensity rise time of benzyl chloride [Fig. 3(a)] seems to be faster than that of toluene [Fig. 3(b)]. This is not because of the liquid macroscopic properties such as surface tension and viscosity, since those coefficients of benzyl chloride are larger than those of toluene. One interpretation will be based on a difference of benzyl radical production dynamics; a direct bond scission

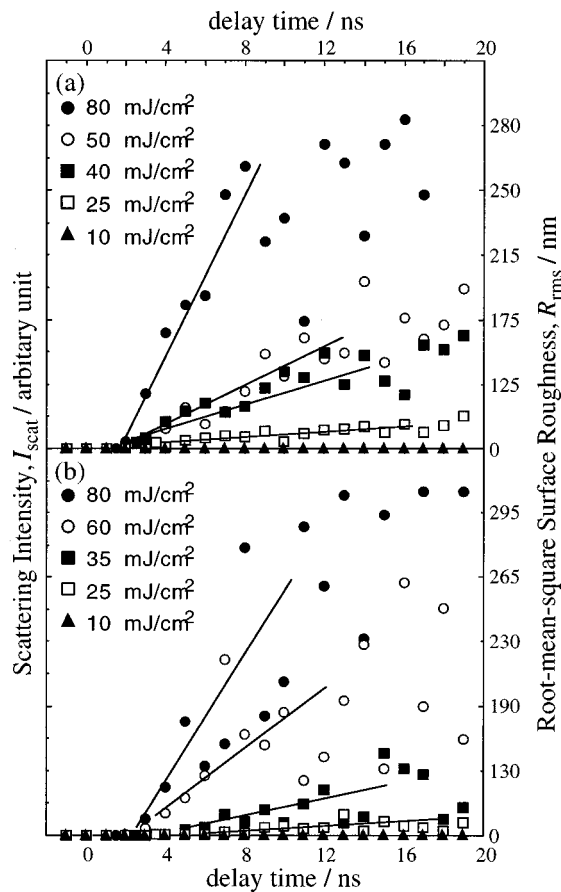


FIG. 3. Fluence dependence of scattering intensity of (a) benzyl chloride and (b) toluene. The left vertical axis represents corrected scattering intensity I_{scat} . The right vertical axis represents the estimated root-mean-square surface roughness R_{rms} .

into benzyl radical will occur in benzyl chloride in the ps time range, while such scission hardly occurs in toluene.⁵

We convert quantitatively I_{scat} to root-mean-square surface roughness R_{rms} , assuming that the scattering is only due to surface roughness in this time domain. The relation between the scattering intensity and surface roughness has been reported as follows by Bennett and Porteus⁸ and Elson *et al.*⁹ under the conditions that R_{rms} is small compared to the probe light wavelength λ and the correlation length in the lateral direction is larger than λ :

$$R_{\text{dif}} = R_0 (4\pi R_{\text{rms}}/\lambda)^2, \quad (1)$$

where R_{dif} is the total diffuse reflectance of a rough surface, and R_0 is the specular reflectance of a perfectly smooth surface of a sample. This model is used to estimate the surface roughness of silicon wafers,¹⁰ for instance. Here, if the backscattering is isotropic to the hemisphere, an equation,

$$I_{\text{scat}} = R_{\text{dif}} \times \text{const}, \quad (2)$$

is valid.

Frosted fused-silica plates ($n_{460}=1.46$, Sigma Koki, DFSQ1-30C02) are used as reference samples for the evaluation of surface roughness. Their R_{rms} are measured by a

stylus profiler [the vertical (lateral) spatial resolution is 1 (500) nm., Sloan, Dektak III] separately, and then correlated to I_{scat} , which are measured here by the present setup. This correlation can be used for estimating the transient R_{rms} of the present liquids, and the R_{rms} value is shown in the right vertical axis of Fig. 3. It is noticeable that the estimated R_{rms} , the standard deviation of surface local height, is in the order of a few hundred nm. In a fs laser ablation, the foil structure on a poly(ethylene terephthalate) film,¹¹ fine ripple structure on a fused-silica plate,¹² and so on, were reported, which were observed by various scanning microscopes; a static observation. A transient surface roughness change induced on an aluminum surface by Nd³⁺:YAG laser irradiation during welding monitored by integrated scattering intensity was reported.¹³ This is, however, the first report on a transient liquid surface roughness induced under the laser ablation condition as far as we know.

In this letter, we describe a time-resolved surface scattering imaging of liquid benzyl chloride and liquid toluene under fs KrF laser ablation conditions. Scattering is induced by surface roughness, which is the initial stage prior to plume ejection, and so on. Furthermore, this experimental method combined with an analysis using a relation of scattering intensity and root-mean-square surface roughness, a quantitative surface roughness estimation was accomplished. Time-dependent evolution from molecular dynamics to macroscopic morphological changes will be elucidated by integrating the present approach, shadowgraphy, and fs transient absorption spectroscopy.⁵

The present work was supported in part by a Grant-in-Aid from the Ministry of Education, Science, and Culture of Japan (09304067) and by Special Coordination Funds for Promoting Science and Technology from the Science and Technology Agency of Japan.

¹L. S. Bennett, T. Lippert, H. Furutani, H. Fukumura, and H. Masuhara, *Appl. Phys. A: Mater. Sci. Process.* **63A**, 327 (1996).

²H. Furutani, H. Fukumura, H. Masuhara, T. Lippert, and A. Yabe, *Appl. Phys. A: Mater. Sci. Process.* **101A**, 5742 (1997).

³M. C. Downer, R. L. Fork, and C. V. Shank, *J. Opt. Soc. Am. B* **2**, 595 (1985).

⁴K. Hatanaka, M. Kawao, Y. Tsuboi, H. Fukumura, and H. Masuhara, *J. Appl. Phys.* **82**, 5799 (1997).

⁵K. Hatanaka, T. Itoh, T. Asahi, N. Ichinose, S. Kawanishi, T. Sasuga, H. Fukumura, and H. Masuhara, *Chem. Phys. Lett.* (in press).

⁶K. Hatanaka, N. Ichinose, S. Kawanishi, T. Sasuga, H. Fukumura, and H. Masuhara, Abstracts of 4th International Workshop on Femtosecond Technology, Tsukuba, Japan, 1997, p. 139.

⁷Y. Tsuboi, K. Hatanaka, H. Fukumura, and H. Masuhara, *J. Phys. Chem. A* **102**, 1661 (1998).

⁸H. E. Bennett and J. O. Porteus, *J. Opt. Soc. Am.* **51**, 123 (1961).

⁹J. M. Elson, J. P. Rahn, and J. M. Bennett, *Appl. Opt.* **22**, 3207 (1983).

¹⁰C. Teichert, J. F. MacKay, D. E. Savage, M. G. Lagally, M. Brohl, and P. Wagner, *Appl. Phys. Lett.* **66**, 2346 (1995).

¹¹J. Heitz, E. Arenholz, D. Bäuerle, R. Sauerbrey, and H. M. Phillips, *Appl. Phys. A: Solids Surf.* **59**, 289 (1994).

¹²J. Ihlemann, B. Wolff, and P. Simon, *Appl. Phys. A: Solids Surf.* **54**, 363 (1992).

¹³H. L. Tardy, Abstracts of Papers Presented at 1987 AWS Convention: 68th American Welding Society Annual Meeting and 18th International AWS Brazing Conference, 1987, pp. 93–94.